Mutational Analysis of the Role of the N Terminus of Actin in Actomyosin Interactions. Comparison with Other Mutant Actins and Implications for the Cross-Bridge Cycle†

Carl J. Miller,‡ Wenise W. Wong,‡ Elena Bobkova,‡ Peter A. Rubenstein,§ and Emil Reisler*,‡

Department of Chemistry and Biochemistry and the Molecular Biology Institute, University of California, Los Angeles, California 90095, and Department of Biochemistry, College of Medicine, University of Iowa, Iowa City, Iowa 52242

Received September 20, 1996; Revised Manuscript Received October 30, 1996⊗

ABSTRACT: Yeast actin mutants with acidic residues at the N terminus either neutralized (DNEQ) or deleted (Δ-DSE) were used to assess the role of N-terminal acidic residues in the interactions of actin with myosin in the contractile cycle. Cosedimentation experiments revealed an ∼3-fold decrease in the binding constant for DNEQ and Δ-DSE actins to myosin subfragment-1 (S1) relative to that of wild type actin both in the presence of MgATP and in the absence of nucleotides (strong binding). DNEQ and Δ-DSE actins protected S1 from tryptic digestion as well as the wild type and rabbit actins. The activation of S1 ATPase by DNEQ and Δ-DSE actins (up to 50 μM) was very low but increased greatly after cross-linking these mutant actins to S1 by dimethyl suberimidate. Thus, the increased dissociation of mutant actins from S1 in the presence of ATP is the main cause for the low acto-S1 ATPase activities. At low-ionic strength conditions and in the presence of methylcellulose, the DNEQ and Δ-DSE actins moved in the *in vitro* motility assays at a mean velocity similar to that of wild type actin (3.0 μm/s). Yet, the sliding velocity of the N-terminal and D24A/D25A and E99A/E100A mutant actins decreased relative to that of the wild type at all levels of external load introduced into the assay and at low densities of heavy meromyosin (HMM) on the cover slip. This indicates a lower relative force generation with the mutant actins. In contrast, the force generated under the same conditions with the 4Ac mutant actin (with four acidic charges at the N terminus) was higher than with wild type actin. At higher-ionic strength conditions (I = 150 mM), the sliding of the DNEQ and Δ-DSE as well as that of the D24A/D25A and E99A/E100A actins ceased even in the presence of methylcellulose, while I341A actin (deficient in strong binding to myosin) still moved. These results indicate the importance of electrostatic actomyosin interactions under physiological salt conditions and show functionally distinct roles for the different myosin binding sites on actin.

Force generation in muscle is thought to depend on transitions between alternating weakly and strongly bound complexes of actin and myosin. An important goal in understanding these transitions is to obtain a detailed description of the actomyosin interface in both the weakly and strongly bound states. This should allow an understanding of the transition between such states and, in turn, facilitate the linking of specific structural properties of both proteins to the kinetic and mechanical cycle of actomyosin. A major advance in muscle biochemistry was the determination of structures for actin and S1 (Kabsch et al., 1990; Rayment et al., 1993a) and the subsequent modeling of the strongly bound actomyosin interface (Rayment et al., 1993b; Schroeder et al., 1993). The area of actin that contributes to the strong binding of myosin is believed to include a hydrophobic patch of residues dominated by α-helix 338−348. In addition, the structural model suggests also an extensive role in myosin binding for several groups of charged surface residues (1−4, 99 and 100, and 24 and 25) on subdomain-1 of actin. Because the structural model of acto-S1 is based on the strongly bound (rigor) complex, it is still not clear how well it can predict the acto-S1 interface in the weakly bound complexes and how closely the weak and strong complexes resemble each other.

The first evidence for a difference in the acto-S1 interface between the weakly and strongly bound complexes was that blocking of residues 1−7 and 18−29 of actin with site-specific antibodies inhibited the weak binding of myosin to actin and the actin-activated myosin ATPase but had only a small effect on the strong acto-S1 binding (DasGupta & Reisler, 1989, 1992; Adams & Reisler, 1993). Mutagenesis of the same sites in *Dictyostelium* actin by substitution of the acidic groups with histidines (Sutoh et al., 1991; Johara et al., 1993) abolished the actin-activated myosin ATPase and the *in vitro* sliding of actin. However, in the presence of methylcellulose, which limits the diffusion of actin from the HMM-coated surface, the *in vitro* motility of yeast actins with charged pairs D24/D25 and E99/E100 substituted with alanine was similar to that of wild type actin (Miller & Reisler, 1995). Clearly, the mild changes of acidic residues

† This work was supported by grants from the United States National Institutes of Health to E.R. (AR22031) and P.A.R. (GM 33689) and from the National Science Foundation to E.R. (MCB9206739) and by USPHS National Research Service Award GM 07185 (C.J.M.).

‡ University of California.

§ University of Iowa.

⊗ Abstract published in *Advance ACS Abstracts,* December 15, 1996.

[1] Abbreviations: DNaseI, deoxyribonuclease I; F-actin, filamentous (polymerized) actin; G-actin, monomeric actin; HMM, heavy meromyosin; S1, myosin subfragment-1; NEM, *N*-ethylmaleimide.

S0006-2960(96)02388-4 CCC: $12.00

24 and 25 and 99 and 100 to alanines do not impair the actomyosin function in the presence of methylcellulose, under the standard low-salt conditions of *in vitro* motility assays.

The sites on actin and myosin which have attracted the most attention are the extreme N terminus of actin and the 50−20 kDa junction of myosin (residues 626−647). The importance and interactions of these regions have been considered in numerous investigations, including cross-linking studies (Sutoh, 1982), immunochemical experiments (Mejean et al., 1987; Miller et al., 1987; DasGupta & Reisler, 1989, 1991, 1992), antipeptide work (Chaussepied & Kasprzak, 1989), and mutational studies on actin (Cook et al., 1992, 1993; Sutoh et al., 1991) and myosin (Uyeda et al., 1994). Despite these studies, important issues related to the functional interaction of these regions remain to be addressed. These include questions on functional differences between charged residues 1−4 on actin and the D24/D25 and E99/E100 pairs and the implication that the former (Sutoh et al., 1991) but not the latter residues (Miller & Reisler, 1995) are critical to actin's motility. Another significant issue is the role of actin's N terminus in the acto-S1 ATPase activity. Work with *Dictyostelium* actin mutants suggested that the N-terminal sequence of actin determines the V_{max} value of acto-S1 ATPase (Sutoh et al., 1991). On the other hand, tryptic cleavage in the 626−647 loop on S1 increased K_m and left V_{max} unchanged (Botts et al., 1982; Bobkov et al., 1996). The interest in these questions is stimulated also by a recent model, in which a key step in the transition from the weakly to strongly bound actomyosin complexes is driven by the charge−charge interaction and stabilization of actin's N terminus and loop 626−647 on myosin. This interaction would lead to a change in the "actin" cleft in the 50 kDa portion of myosin (Holmes, 1995; Miller et al., 1995; Brenner et al., 1996) and to the subsequent power stroke.

Here, we have assessed the functional role of the actin N-terminal 1−4 segment in the contractile cycle by observing the actomyosin interactions with actins completely devoid of the N-terminal charges. We show that in analogy to the case for D24/D25 and E99/E100 sites on actin the N terminus is essential for the sliding function of actin over myosin under physiological ionic strength conditions but not at low-salt conditions. Yet, all of these mutants generate less force with myosin under low-salt conditions than wild type actin. The N-terminal actin residues contribute to acto-S1 binding in both the weakly and strongly bound states, while the D24/D25 and E99/E100 sites are involved only in the weak binding of actomyosin. These results and the comparison with other mutant actins allow the classification of four sites in subdomain-1 of actin according to their binding to myosin and contribution to specific steps of the cross-bridge cycle.

MATERIALS AND METHODS

Preparation of Proteins. Yeast actin was isolated from each strain using DNaseI affinity chromatography as previously described (Cook et al., 1993). Rabbit actin and myosin were prepared from rabbit skeletal muscle according to the methods of Spudich and Watt (1971) and Godfrey and Harrington (1970), respectively. Myosin subfragment-1 was prepared according to Weeds and Pope (1977).

Cosedimentation Assays. Cosedimentation assays of the weak binding of S1 to 4.0 μM phalloidin-stabilized actin were carried out at 23 °C in 3.0 mM ATP, 3.0 mM $MgCl_2$, 5.0 mM KCl, and 10 mM imidazole at pH 7.4 as previously described (Miller & Reisler, 1995). ATP was added after the incubation of proteins for 10 min. The concentrations of S1 ranged between 5.0 and 40.0 μM. The protein samples were centrifuged at room temperature in a Beckman airfuge at 140000*g* for 10 min. Similar assays, except for a longer centrifugation (20 min) and the absence of MgATP, were done for the strong binding of S1 (1.0−10.0 μM) to actin (4.0 μM) in the presence of 100 mM KCl, 4.0 μM phalloidin, and 10 mM imidazole at pH 7.4. Under these conditions, S1 was not pelleted when centrifuged in the absence of actin. The choice of different salt conditions for the weak and strong acto-S1 binding assays was dictated by the experimental need to increase the weak and decrease the strong binding of S1 to actin. Resuspended pellets and supernatants of each sample were examined by SDS−PAGE (Laemlli et al., 1970). Gels were stained with Coomassie Blue, and the bands were quantified by a Biomed Instruments softlaser densitometer (Fullerton, CA) interfaced to an IBM-compatible 486 computer for integration of peak areas. The densitometric traces of pelleted protein bands were analyzed to determine the molar ratios of S1 bound to actin. Molar stain ratios for S1 and actin were obtained from appropriate calibration gels.

Protection of Loop 626−647 in S1 by Actin against Tryptic Digestion. All digestions were performed in 40 mM NaCl, 10 mM imidazole, and 2.5 mM $MgCl_2$ at pH 7.0 with 5 μM S1 and 15 μM actin. As shown by pelleting experiments, the 3-fold molar excess of actin over S1 was needed to assure full binding (>90%) of S1 to all actins. Free S1 was digested as a control. Reaction mixtures were held at 25 °C, and digestions were started with the addition of trypsin at a weight ratio of 50/1 (S1/trypsin). At given time intervals, aliquots were removed from the proteolytic reaction mixtures and were mixed with soybean trypsin inhibitor (3 × the trypsin concentration, w/w) to stop the digestions. Catalase was added to all samples as an internal standard. The denatured samples were analyzed by SDS−PAGE on discontinuous gels (10 and 15% w/v). The optical densities of the Coomassie Blue-stained protein bands were determined with the Biomed gel scanner. Rates of digestion of loop 626−647 on S1 were obtained by quantifying the decay of the combined 95 and 70 kDa S1 bands on SDS gels as a function of reaction time and fitting the data to a single-exponential expression (Duong & Reisler, 1987).

Actin-Activated S1 ATPase Assays. Actin-activated ATPase activity was measured at 25 °C by using the malachite green assay (Kodama et al., 1986). Due to assay sensitivity, free phosphate was removed from actin stock solutions as described before (Sutoh et al., 1991). Actin samples at final concentrations from 2 to 50 μM were preincubated with 0.4 μM S1 for 20 min in the ATPase buffer (5 mM KCl, 2 mM $MgCl_2$, and 10 mM imidazole at pH 7.4). The ATPase reaction was initiated by the addition of ATP to a 1 mM final concentration. The reactions were stopped with an equal volume of 0.6 M perchloric acid and then the mixtures diluted appropriately while maintaining a final concentration of 0.3 M perchloric acid. The mixtures were centrifuged at 14 000 rpm for 10 min in a microcentrifuge to remove precipitated proteins. The amounts of released phosphate were determined and corrected for the activity of S1 alone as reported before (Kodama et al., 1986).

Cross-Linking of F-Actin−S1 Complexes. Actins were cross-linked to S1 by dimethyl suberimidate (DMS) according to the methods of Labbe et al. (1982). The filamentous form of each actin (1.0 mg/mL) and S1 (1.0 mg/mL) were incubated in 40 mM triethanolamine hydrochloride at pH 8.3 for 30 min. Cross-linking of the acto-S1 complexes was initiated upon addition of dimethyl suberimidate (0.8 mg per 1 mg of protein) which had been dissolved immediately prior to use. Reaction aliquots were removed along the time course of the reaction, and the cross-linking was stopped with glycine (200 mM). Actin-activated ATPase of the cross-linked species was determined as described above with the following changes. Samples were removed from the cross-linked mixtures after stopping the reaction and diluted 20-fold in the ATPase buffer to a final S1 concentration of 0.05 mg/mL. After 20 min of incubation, the ATPase reaction was initiated by the addition of 1.0 mM ATP, and the amount of phosphate liberated was determined as above.

In Vitro Actin Motility Assays. The motility assays were performed as previously described (Miller et al., 1996). The temperature was maintained at 25 °C for all assays. HMM was prepared as described by Kron et al. (1991). To remove ATP-insensitive heads, HMM was centrifuged with 0.15 mg/mL phalloidin-stabilized actin in a solution containing 0.1 M KCl, 4.0 mM $MgCl_2$, and 3.0 mM MgATP for 20 min in a Beckman airfuge. The supernatant was applied to nitrocellulose-treated cover slips at an HMM concentration of 0.2 mg/mL, unless stated otherwise. Rhodamine phalloidin-labeled actin filaments were added to the coated cover slips at 10 nM, and after 30 s, the unbound filaments were washed away with the assay buffer (25 mM KCl, 1 mM EGTA, 4 mM $MgCl_2$, 10 mM dithiothreitol, and 10 mM imidazole at pH 7.4). The ionic strength of the high-salt buffer was adjusted to 150 mM with KCl. Movement was initiated with the assay buffer containing 1 mM ATP and an oxygen-scavenging system. Quantification of the sliding velocities was done with an Expertvision system (Motion Analysis, Santa Rosa, CA). The velocities of individual filaments with standard deviations of less than $^1/_3$ of the average velocity were used for statistical analysis (Homsher et al., 1991) and were considered to move smoothly in the assay system.

NEM−HMM was prepared as described previously (Warrick et al., 1993). The *in vitro* motility assay was performed as above with the following modifications. HMM and NEM−HMM at appropriate weight ratios were adsorbed to the assay surface for 2 min and washed off with 6 volumes of assay buffer to prevent contamination with NEM−HMM. Nonmoving filaments were determined by tracking the centroid of each filament image with the Expertvision system and charting its movement for 20 s.

RESULTS

The interactions with myosin of mutant yeast actins that lack the two negatively charged residues present at the N terminus of the wild type yeast actin sequence (versus the four charges present in rabbit α-actin) were examined and compared with the interactions of other mutant actins. The N-terminal sequences of yeast actins used in this work were the following (Figure 1): wild type actin, Ac-Met-Asp-Ser-Glu-Val...; 4Ac actin, Ac-Met-Asp-Glu-Asp-Glu-Val...; DNEQ, Ac-Met-Asn-Ser-Gln-Val...; and (Δ-DSE, ^+H_3N----------Val.... These actins were previously shown to support growth as the sole actin in the yeast cell and to produce functional actin *in vitro* (Cook et al., 1992; Crosbie et al., 1994). Here, we use these mutants to better establish the role of the N-terminal residues in the interactions of actin with myosin. Other mutant actins used in this work (Figure 1) and employed in previous studies included the weak binding mutants D24A/D25A and E99A/E100A (Miller et al., 1995) and the strong binding site mutant I341A (Miller & Reisler, 1996).

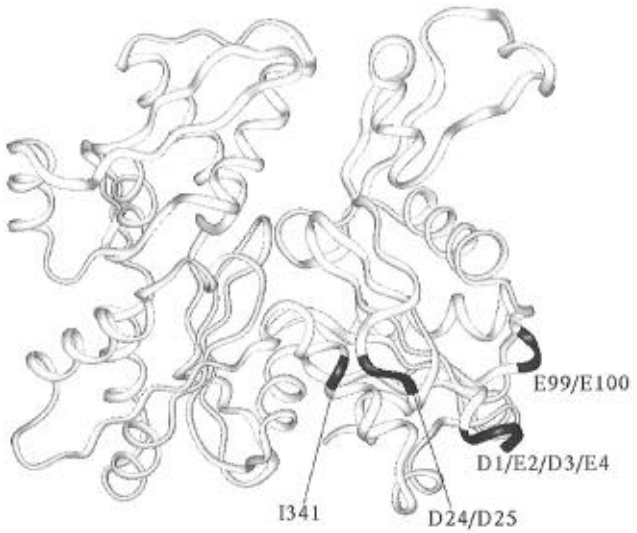

FIGURE 1: Location of the mutated amino acid residues on the G-actin structure (displayed by Insight II) of Kabsch et al. (1990).

Rigor and ATP-Sensitive Binding of Mutant Actins to S1. The affinities of mutant actins for S1 in both the absence and presence of ATP were tested in cosedimentation experiments. The data for the binding of S1 to wild type actin in the absence of nucleotides could be represented by a curve corresponding to a K_a of $(1.8 \pm 0.2) \times 10^6$ M^{-1} (Figure 2, solid curve). Calculated binding curves describing the binding data for S1 and DNEQ [$K_a = (0.7 \pm 0.5) \times 10^6$ M^{-1}, dashed curve] and Δ-DSE [$K_a = (0.4 \pm 0.5) \times 10^6$ M^{-1}, dotted curve] mutant actins indicated a decrease in their affinity to S1 relative to the wild type actin value. The binding of S1 to 4Ac mutant actin was similar [$K_a = (1.7 \pm 0.2) \times 10^6$ M^{-1}] to that to wild type actin (data not shown). In the presence of 3.0 mM MgATP, a similar 3-fold difference was observed between the binding of S1 to wild type [$K_a = (4.6 \pm 0.1) \times 10^4$ M^{-1}, Figure 3, solid curve] and to the N-terminal DNEQ and Δ-DSE mutant actins [$K_a = (1.6 \pm 0.1) \times 10^4$ M^{-1} , Figure 3, dashed curve]. An earlier study detected no significant difference in the binding of S1 to 4Ac and wild type actin in the presence of MgATP (Cook et al., 1993). The new results with DNEQ and Δ-DSE mutant actins indicate that the two charged residues at the N terminus of wild type actin play a role in the binding of actin to myosin in both the presence and absence of ATP. The binding contribution of the N-terminal charged residues appears to saturate with the presence of two acidic groups at the N terminus.

Protection of Loop 626−647 (50−20 kDa Junction) in S1 by Mutant Actins against Tryptic Cleavage. The cosedimentation experiments revealed a role, albeit limited, of the actin N-terminal acidic residues in the rigor binding of myosin. The binding of actin's N terminus to lysine residues in loop 626−647 on S1 was inferred in previous studies from

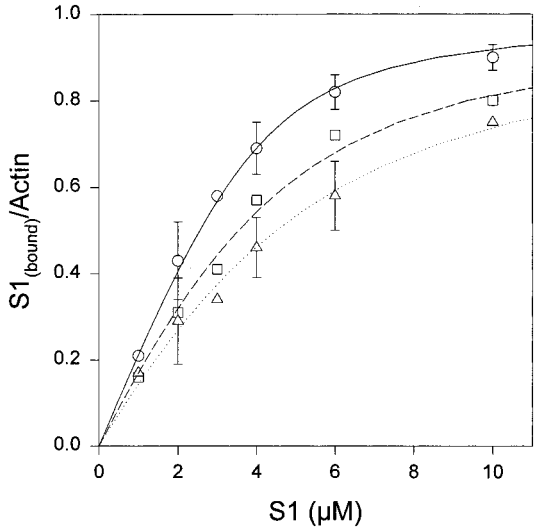

FIGURE 2: Binding of S1 to wild type and mutant actins under rigor conditions. Mixtures of F-actin (4.0 μM) and S1 (between 1.0 and 10.0 μM) were preincubated in 100 mM KCl, 4.0 μM phalloidin, and 10 mM imidazole at pH 7.4 and 22 °C and then pelleted in a Beckman airfuge. Supernatants and resuspended pellets were run on SDS−PAGE and quantified by densitometry. The molar ratios of S1 bound to wild type actin (○) are described by a single calculated binding curve (solid curve) corresponding to a K_a of $(1.8 \pm 0.2) \times 10^6$ M^{-1}. The calculated binding curves describe the binding of S1 to DNEQ [□, $K_a = (0.7 \pm 0.5) \times 10^6$ M^{-1}, dashed curve] and Δ-DSE actin [△, $K_a = (0.4 \pm 0.5) \times 10^6$ M^{-1}, dotted curve]. Error bars represent the mean deviation from three independent experiments.

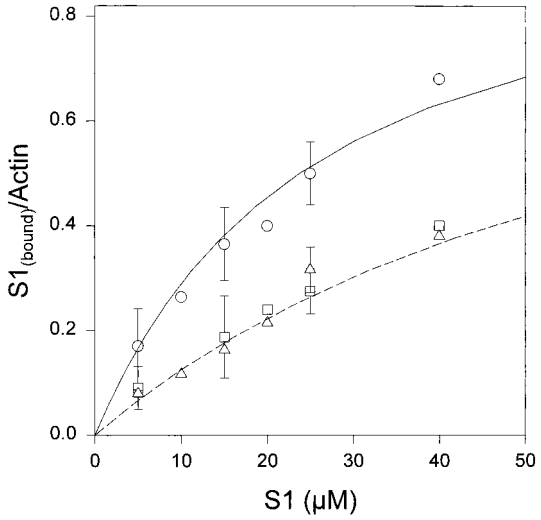

FIGURE 3: Binding of S1 to wild type and mutant actins in the presence of MgATP. Mixtures of F-actin (4.0 μM) and S1 (between 5.0 and 40 μM) were pelleted in a Beckman airfuge at 140000*g* for 10 min in a solvent containing 5.0 mM KCl, 1.0 mM EDTA, 3.0 mM MgATP, 4.0 μM phalloidin, and 10 mM imidazole at pH 7.4 and 22 °C. Supernatants and pelleted samples were run on SDS−PAGE and quantified by densitometry. The molar ratios of S1 bound to wild type F-actin (○) are described by a single calculated curve corresponding to a K_a of $(4.6 \pm 0.1) \times 10^4$ M^{-1} (solid curve). The calculated binding curve corresponding to a K_a of $(1.6 \pm 0.1) \times 10^4$ M^{-1} (dashed curve) describes the binding of S1 to DNEQ (□) and Δ-DSE (△) actin. Error bars represent the mean deviation from three independent experiments.

cross-linking (Sutoh, 1982) and proteolytic digestion of acto-S1 (Mornet, 1979; Yamamoto, 1979). A test of such specific interaction is based on the ability of actin to protect loop 626−647 from tryptic cleavage. Normal tryptic treatment of myosin in the absence of actin yields three stable

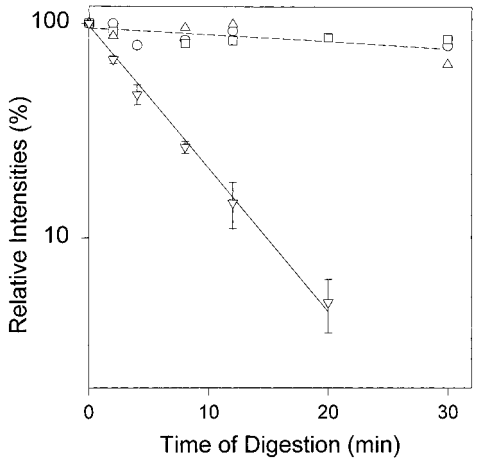

FIGURE 4: Protection of tryptic digestion of S1 by mutant and wild type actins. The ability of each actin (15 μM) to protect the 50−20 kDa junction on S1 (5 μM) from tryptic digestion was measured in a buffer containing 40 mM NaCl, 2.5 mM $MgCl_2$, and 10 mM imidazole at pH 7.0. Semilogarithmic plots of the combined relative intensities of the 95 and 70 kDa bands on SDS gels versus time of digestion are shown for S1 cleavage in the absence of actin (▽, solid line) and in the presence of wild type (○), DNEQ (□), and Δ-DSE (△) actins (dashed line). The corresponding rates of cleavage are 0.14 min^{-1} for the solid line and 0.005 min^{-1} for the dashed line.

Table 1: Protection of Loop 626−647 in S1 from Tryptic Cleavage by Actin[a]

actin	protection of loop (%)
rabbit α-actin	100
yeast wild type	95.4 ± 1.7
yeast DNEQ	90.4 ± 10.6
yeast Δ-DSE	101 ± 1.4

[a] The rate of cleavage of loop 626−647 in S1 in the presence of rabbit skeletal α-actin was used as a reference state for 100% protection of the loop in each set of experiments. The rate of free S1 cleavage in the same set was taken as a reference state for 0.0% protection of the loop. The errors represent an average of three sets of experiments.

fragments: the 25, 50, and 20 kDa peptides. However, in the presence of actin, the 50 kDa product, which is visible in the absence of actin, does not appear on gels and the 70 and 25 kDa bands that result from tryptic cleavage at the 25/70 kDa site are the main reaction products. Thus, the rate of loop 626−647 cleavage, or its protection relative to free S1, can be quantified by monitoring the combined amounts of the undigested 95 kDa (intact S1) and the 70 kDa fragment present in the sample as a function of digestion time (Duong & Reisler, 1987). Figure 4 shows that the rate of digestion of loop 626−647 is slowed in the presence of wild type actin (0.005 min^{-1}) by about 30-fold in comparison to the rate in the absence of actin (0.14 min^{-1}). Strikingly, the DNEQ and Δ-DSE mutant actins protected S1 from tryptic digestion as well as the wild type actin (Figure 4, Table 1). These results indicate that, at least in the rigor complex, the 626−647 loop either is sterically blocked by actin or assumes a protease-insensitive conformation, regardless of the presence or absence of the charges on the N terminus of actin. The high amounts of mutant actins required to form the actomyosin complex in the presence of MgATP preclude similar digestion experiments under weak-binding conditions.

Actin-Activated ATPase Activities. A greatly reduced actin-activated ATPase of S1 was found before for both the

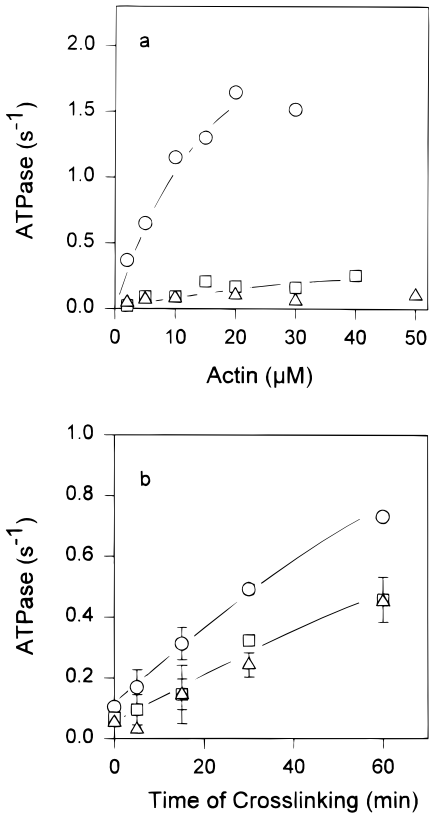

FIGURE 5: Actin-activated ATPase activities of S1 in the presence of wild type and mutant actins. (a) The activation of S1 ATPase by each actin was measured at 25 °C in the presence of between 2.0 and 50.0 μM phalloidin-stabilized F-actin, 0.4 μM S1, and 1 mM ATP in an assay buffer containing 2.0 mM $MgCl_2$, 5.0 mM KCl, and 10 mM imidazole at pH 7.4. The ATPase rates in the presence of wild type actin (○) are described by the upper hyperbola; the rates determined in the presence of DNEQ (□) and Δ-DSE (△) are described by the lower set of data. (b) The activation of S1 ATPase by each actin was measured for the mixtures of S1 and wild type and mutant actins as a function of cross-linking time with dimethyl suberimidate. The activities were measured at 0.5 μM S1 and 1 mM ATP in an assay buffer containing 2 mM $MgCl_2$, 5 mM KCl, and 10 mM imidazole at pH 7.4. The ATPase rates are for S1 cross-linked to wild type actin (○), DNEQ actin (□), and Δ-DSE actin (△).

DNEQ and Δ-DSE mutant actins at a single actin concentration (20 μM) (Cook et al., 1992). Similar low activities were observed also in this work, at up to 50 μM actin (Figure 5a), precluding the determination of the K_m and V_{max} values of acto-S1 ATPase. To assess the effect of N-terminal actin mutations on these parameters and to maximize the interaction of the two proteins in the presence of ATP, the acto-S1 complexes were cross-linked by dimethyl suberimidate. Such a cross-linking of the rabbit skeletal acto-S1 complex increased its ATPase activity to close to the V_{max} value (Labbe et al., 1982). SDS−PAGE analysis of the cross-linked S1 and yeast actins revealed similar cross-linking of S1 (up to 15%) to wild type and mutant actins over the 60 min of reaction time (data not shown). In parallel, the ATPase activities of the acto-S1 complexes increased sharply with time of reaction (Figure 5b). The complex of wild type actin and S1 resulting from a 60 min cross-linking reaction had an actin-activated S1 ATPase activity of 0.7−0.8 s^{-1} compared to 0.1 s^{-1} for the un-cross-linked sample. Similarly, DNEQ and Δ-DSE actin-activated S1 ATPase activities also showed a large increase, with rates approaching 0.4 or 0.5 s^{-1} for the cross-linked compared to 0.05 s^{-1} for the un-cross-linked acto-S1. This result suggests that the low activities of the un-cross-linked acto-S1 were largely due to a decreased affinity of mutant actins for S1 in the presence of ATP. Thus, a primary role of the two N-terminal charged residues on yeast actin is to contribute to the weak binding with myosin. However, the reduced levels of activity at all times of cross-linking indicate that these mutants are also catalytically deficient and their complexes with S1 might hydrolyze ATP at V_{max} values roughly $^1/_2$ of that with wild type actin.

Table 2: Sliding of Mutant Actin Filaments in the *in Vitro* Motility Assay[a]

	sliding of yeast actin mutants (μm/s)					
ionic strength	WT	DNEQ	Δ-DSE	D24A/ D25A	E99A/ E100A	I341A
50 mM	3.0	2.8	3.0	2.9	3.0	2.0
150 mM	3.2	−	−	−	−	2.3

[a] The motilities of actin filaments were measured as described in Materials and Methods. At least 100 filaments were analyzed for each sample. The standard deviation of the mean values was 0.2 μm/s. No directed movement of DNEQ, Δ-DSE, D24A/D25A, and E99A/E100A actin filaments was detected in the high-ionic strength assays. WT, wild type.

Sliding of Actins in the in Vitro Motility Assays. The ability of the DNEQ and Δ-DSE actin filaments to slide over skeletal muscle heavy meromyosin (HMM) was tested in the *in vitro* motility assay. Strikingly, at standard-ionic strength conditions (I = 50 mM), both the DNEQ (V_s = 2.8 ± 0.3 μm/s) and the Δ-DSE actins (V_s = 3.0 ± 0.4 μm/s) moved in a manner identical to that of wild type actin (V_s = 2.9 ± 0.3 μm/s, Table 2). However, this sliding was dependent on the presence of methylcellulose in the assay buffer. In the absence of this viscosity-enhancing agent, the filaments dissociated from the assay surface upon addition of MgATP. This behavior was previously observed for mutant actins with charged residues D24/D25 and E99/E100 changed to alanine. These two mutant actins showed a decreased binding to myosin in the presence of MgATP (Miller & Reisler, 1995), both in the motility assays and in equilibrium binding experiments, which was similar to that observed for DNEQ and Δ-DSE actins in this study. However, in contrast to that for the N-terminal mutants, the binding of S1 to the D24/D25 and E99/E100 mutants in the absence of MgATP was similar to that to wild type actin.

It has been suggested that the charged residues in subdomain-1 of actin discussed above are only important at nonphysiological low-salt conditions used in solution work and the *in vitro* motility assays (Holmes, 1995), where screening of the electrostatic actomyosin interaction by salt is very limited. To address this possibility, the *in vitro* motilities of actin mutants were monitored also under conditions approaching physiological ionic strength (I = 150 mM). In contrast to the normal motion of the wild type actin, both the DNEQ and the Δ-DSE mutants were unable to slide at these conditions after the addition of ATP (Table 2). Despite their ATP-sensitive interaction with the HMM surface, DNEQ and Δ-DSE actin filaments showed only slight random motion with no evidence of myosin-directed sliding. To verify that the loss of sliding in N-terminal mutants resulted from a decrease in the weak binding, we tested the effect of higher ionic strengths on a mutant deficient in the strong binding (I341A; Miller et al., 1996)

Table 3: Effects of HMM Concentration on the Sliding of Mutant Actin Filaments in the *in Vitro* Motility Assays (I = 50 mM)[a]

HMM (mg/mL)	sliding of yeast actin mutants (μm/s)					
	WT	DNEQ	D24A/D25A	E99A/E100A	I341A	4Ac
0.5	3.0	3.0	2.9	3.0	2.0	3.1
0.1	3.1	2.4	2.3	2.5		3.2
0.06	2.5	2.0	1.5	1.8	−	2.8
0.03	1.7	−	−	−		2.0
0.015	−					1.2

[a] The motilities of actin filaments were measured as described in Materials and Methods. At least 50 filaments were analyzed for each sample. The standard deviation of the mean values was between 0.1 and 0.3 μm/s. The sliding velocities of Δ-DSE actin were the same as those of DNEQ actin. The concentrations of HMM are for solutions used for adsorption of HMM to cover slips.

Table 4: Effect of NEM−HMM on the Sliding of Mutant Actin Filaments in the *in Vitro* Motility Assays (I = 50 mM)[a]

NEM−HMM/HMM	percentage of yeast mutant actin filaments sliding in the assays				
	WT	DNEQ	D24A/D25A	I341A	4Ac
0	98	90	88	67	95
0.05	75	60	54	35	90
0.11	47	24	25	−	75
0.17	28	−	−		60
0.25	−				35
0.33					−

[a] The motilities of actin filaments were measured as described in Materials and Methods. At least 100 filaments were analyzed for each sample. The sliding of Δ-DSE and E99A/E100A actins was the same as that of DNEQ and D24A/D25A actins. NEM−HMM/HMM is given as molar ratios of modified to unmodified HMM in solutions used for adsorption of HMM to cover slips.

as well as on other mutant actins deficient in the weak binding to myosin (D24A/D25A and E99A/E100A; Miller & Reisler, 1995). The sliding of the I341A mutant, which moves slower than the wild type, was relatively unaffected by the increase in ionic strength. In contrast, the D24A/D25A and E99A/E100A mutant actins behaved in a manner similar to that of the DNEQ and Δ-DSE actins and did not slide at the higher-ionic strength conditions.

Movement of Mutant Actins against Load and over Diluted HMM. We have shown in a recent study (Miller et al., 1996) that a 10-fold decrease in the strong binding of myosin to actin (for the I341A mutant) inhibits markedly the sliding velocities (see also Table 2) and the number of sliding mutant actin filaments. Yet, despite a small decrease (3-fold) in the strong binding of myosin for the N-terminal mutants and none for the D24/D25 and E99/E100 mutants, their sliding properties were identical in both low- and high-salt conditions. To improve the resolution of motility assays and to better compare these mutants, their movement was observed over diluted HMM and under conditions providing an estimate of relative forces generated by HMM and the various actins (i.e., in the presence of external load). Actin sliding stops in such assays when the HMM concentrations are decreased to the point at which the number of force-generating cross-bridges is insufficient to sustain motion and/or overcome the small intrinsic load of the assays (due to adsorption or photodamage of HMM). Motility experiments with different HMM concentrations used for coating the cover slips showed the same dependence of DNEQ, D24A/D25A, and E99A/E100A mutant actin movement on HMM (Table 3). Directed movement was detected for these mutant actins over HMM only at concentrations of ≥0.06 mg/mL, while the wild type actin was able to slide with HMM diluted to 0.03 mg/mL. Strikingly, the 4Ac mutant actin could slide at lower HMM concentrations than wild type actin. The strong binding deficient mutant (I341A) stopped moving at higher HMM concentrations than other actins (Table 3).

The relative forces generated by HMM with yeast mutant and wild type actins were tested by observing the sliding of actin over HMM mixed with increasing amounts of load-bearing NEM-modified HMM. This approach has been previously used for measuring the relative force generation by smooth muscle and skeletal muscle myosins (Haeberle, 1994) and more recently for the comparison of force generation by HMM with the wild type and I341A mutant actins (Miller et al., 1996). The sliding of the I341A actin, deficient in the strong binding to myosin, was stopped at a lower NEM−HMM/HMM ratio than that required for stopping wild type actin filaments. We used the same approach to assess the relative force generated by the N-terminal, D24/D25, and E99/E100 mutant actins and observed that, at all ratios of NEM−HMM (external load) to HMM, fewer mutant actin filaments moved than did wild type actin filaments. Mutant actin filaments moved up to but not at a ratio of 0.17 NEM−HMM/HMM, while the wild type filaments moved at ratios up to 0.25 (Table 4). Strikingly, a 0.33 molar ratio of NEM−HMM/HMM was required for stopping the sliding of the 4Ac mutant actin (Table 4). These ratio values, at which the motion of actin is stopped, yield an approximate ratio of forces developed by HMM and actins of ∼0.7/1.0/1.3 for the weak site mutants the wild type/the 4Ac mutant. Mutant actin filaments which lost two acidic residues, either at the N terminus or in loops 21−29 and 92−103, generate less force than the wild type actin. Thus, as in other motility assays, these mutants are indistinguishable from each other but clearly different from the 4Ac and I341A mutant actins.

DISCUSSION

Previous studies had identified three anionic sites on subdomain-1 of actin as being important in the weak binding interaction between actin and myosin: (1) the N-terminal acidic residues, (2) D24/D25, and (3) E99/E100 (Sutoh et al., 1991; Johara et al., 1993; Cook et al., 1993; Miller & Reisler, 1995). Although those studies were concerned with the role of the three sites in the interaction of actin with myosin, several important aspects of this problem were not addressed. The focus of this work was determining if there were functional differences among these sites in terms of weak binding, strong binding, activation of the myosin ATPase activity, and the ability of myosin to move actin in the presence of load and at physiological-ionic strength conditions.

Binding Interactions. In the presence of ATP, removal of negative charges from each of the three sites produced similar small changes in the "weak" acto-S1 interaction and a similar requirement for methylcellulose for actin motility under low-salt conditions. These observations are consistent with the previously determined electrostatic nature of the weakly bound complexes (Chalovich et al., 1984).

In contrast, these sites do seem to behave differently under "strong" binding conditions in the absence of ATP. Removal

Scheme 1

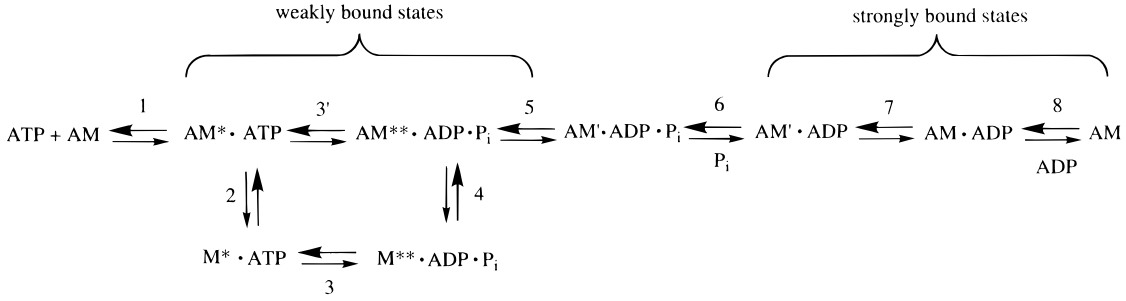

of the two N-terminal acidic residues in wild type yeast actin resulted in a small decrease in the strong binding interaction. This decrease did not affect the movement of actin in the *in vitro* motility assay under low-salt conditions and at high HMM concentrations. Our previous work showed that the D24/D25 and E99/E100 charges were not important for the binding to actin in the absence of ATP (Miller & Reisler, 1995). Our results suggest that in the rigor, but probably not in the weak complex, the N-terminal acidic residues are functionally distinct from those at the other two sites. Furthermore, these results indicate a role for the N-terminal acidic residues throughout the cross-bridge cycle, although the contribution of these residues to the formation of the strong complex is not essential for force generation. Additionally, experiments with the 4Ac mutant indicate that two acidic N-terminal residues appear to be sufficient to saturate the contribution of this site to the binding of actin to myosin under both strong binding (this paper) and weak binding conditions (Cook et al., 1993).

The interaction of actin's N terminus with loop 626−647 on myosin is believed to involve the binding of actin's acidic residues to the cluster of lysines in the myosin loop. The main support for such an interaction includes the cross-linking of actin's N terminus to the myosin loop by carbodiimide (Sutoh, 1982) and the protection of the loop by actin from tryptic cleavage (Mornet et al., 1979). Our results shed new light on this interaction. The fact that mutant actins without acidic N-terminal residues still protect the myosin loop from tryptic digestion suggests that this loop is folded and/or buried in the actomyosin complex. Clearly, such rearrangement of the loop does not require its binding to acidic residues in actin's N terminus, at least not in the strongly bound complexes. Yet, it is possible that the interaction of actin's N terminus with myosin's loop 626−647 facilitates the folding of this loop during the transition from weakly to strongly bound complexes in the cross-bridge cycle (Holmes, 1995; Miller et al., 1995; Brenner et al., 1996). Such a possibility is supported by previous (Cook et al., 1993) and present acto-S1 ATPase measurements.

Activation of Myosin ATPase Activity. Cook et al. (1993) previously showed that doubling the net charge on the yeast actin N terminus to 4, to make it equivalent to that of muscle α-actin, increased the V_{max} of the acto-S1 ATPase. Here, we demonstrated that removal of the original two charges of wild type yeast actin decreased ATPase activation. Much of this activation was recovered upon cross-linking the actin to S1. These results show that the N-terminal acidic residues play an important part in the activation of myosin ATPase and that much, but not all, of the decrease seen here for the un-cross-linked actin can be attributed to a decreased weak binding interaction. A catalytic function of these residues is indicated also by the fact that a 3-fold decrease in weak binding is not sufficient to account for the large decrease in ATPase activation. Additionally, the results with the 4Ac mutant demonstrate that, while two charges saturate binding requirements, they are not enough to saturate the catalytic function.

Table 5: Effect of NEM−HMM on the Sliding of Mutant Actin Filaments in the *in Vitro* Motility Assays (I = 50 mM)[a]

NEM−HMM/HMM	sliding velocities of yeast mutant actin filaments in the motility assays				
	WT	DNEQ	D24A/D25A	I341A	4Ac
0	3.1	3.0	2.8	2.0	2.9
0.05	2.6	1.9	2.0	1.2	2.6
0.11	2.1	1.3	1.1	−	2.5
0.17	1.3	−	−		1.8
0.25	−				1.5
0.33					−

[a] The motilities of actin filaments were measured as described in Materials and Methods. At least 100 filaments were analyzed for each sample. The standard deviation of the mean values was between 0.1 and 0.3 μm/s. The sliding of Δ-DSE and E99A/E100A actins was the same as that of DNEQ and D24A/D25A actins.

The rate-limiting step of the actin-activated ATPase is thought to be step 5 in Scheme 1 [adopted from Ma and Taylor (1994)], i.e., a transition of the low-affinity actin·myosin·ADP·P_i (A·M**ADP·P_i) to an activated, higher-affinity A·M′·ADP·P_i complex (conformationally strained, ready for the power stroke; Regnier et al., 1995; Lymn & Taylor, 1971; Taylor, 1979; Ma & Taylor, 1994; Lionne et al., 1995). We propose that the N terminus of actin facilitates this transition by interacting with the 626−647 loop on myosin. However, as shown by *in vitro* motility experiments under low-salt conditions (Tables 3 and 5), the down (in DNEQ and Δ-DSE)- or up-modulation (in 4Ac) of the A·M**ADP·P_i to A·M′·ADP·P_i transition does not impact the velocity of actin motion at unloaded conditions and at high HMM concentrations. Under such conditions, motility is rate-limited by subsequent steps in the cross-bridge cycle.

In Vitro Motility: Low and High-Salt Conditions. Our observed wild type behavior of the DNEQ and Δ-DSE mutants in the motility assay in low salt and at saturating HMM concentrations is in contrast to previous reports that substitution of two of the three N-terminal acidic residues of *Dictyostelium discoideum* actin with histidines caused a large decrease in sliding velocities (Sutoh et al., 1991). Several factors can contribute to the differences in our findings. (1) The introduction of large positively charged residues might be more inhibitory than the deletion of these residues or replacement with isosteric neutral residues that we carried out. (2) The motility of the *Dictyostelium* mutant actins was measured at 22.5 °C, although it has been

observed that they move better at 30 °C. Possibly, these actins are more temperature-sensitive than our mutants. (3) Methylcellulose, required for the movement of our weak binding mutants, was not used in the *Dictyostelium* study.

The low-ionic strength conditions used in most of the *in vitro* motility assays and in solution experiments on acto-S1 interactions raised an important question about the physiological significance of the results concerning the electrostatic component of these interactions. Kraft et al. (1996) recently showed using intact muscle fibers that caldesmon, an inhibitor of weak actomyosin binding, inhibited the active force even at a 170 mM ionic strength. The loss of sliding of all of our weak binding mutants at a 150 mM ionic strength is consistent with their result. This loss of function indicates that at a higher ionic strength the overall weak actomyosin binding decreases to a point at which the individual contribution of each one of the three groups of charged residues on yeast actin is required for filament sliding even in the presence of methylcellulose. Conversely, when electrostatic interactions between myosin and actin are enhanced by low-salt conditions and saturating HMM concentrations, the loss of any one of these charge groups does not inhibit actin motility. For yeast actin, these results suggest but do not prove yet that what determines whether HMM enters the force-producing states of the cross-bridge cycle via the weakly bound states is the net charge density on subdomain-1 of actin and not a specific, single set of charged residues.

Relative Forces and Cross-Bridge Cycle Considerations. Performing the motility assays over an increased range of HMM concentrations and in the presence of load allowed us to resolve differences between the wild type, 4Ac, and weak binding mutants that were not apparent under the standard assay conditions. All three types of weak binding mutants with a reduced number of acidic residues displayed virtually the same decrease in the force generated against the NEM−HMM load relative to wild type actin in terms of slower velocities and a lower fraction of filaments capable of sliding. These effects must be accommodated by changes in the cross-bridge cycle (Scheme 1). Such changes may involve either a reduced population of force-generating cross-bridges or a lower force-produced per single cycle. Although the latter possibility cannot be excluded without unitary force measurements, the former option is favored because higher concentrations of HMM are required for the weak binding sites mutants than for WT actin to produce similar motilities (Table 3). Given virtually identical rigor binding of S1 to wild type, D24A/D25A, and E99A/E100A actins (Miller et al., 1995), the decrease in the population of strongly bound (force-generating) cross-bridges for these mutants and the N-terminal mutants probably arises from a lower population of the weakly bound complexes. Thus, fewer HMM cross-bridges reach the isomerization step (step 5 in Scheme 1) with the mutant actins than with WT actin. Also, as shown here and previously, the V_{max} values for the three types of actins are probably reduced, indicating a decreased isomerization (in step 5 of Scheme 1) and thus a further decrease in the flux of cross-bridges through the cycle into the strongly bound states. On the basis of these results, the functional defect in all these cases stems from less favorable equilibria in steps 2, 4, and 5 of Scheme 1, i.e., from a decreased population of weakly bound states, decreased isomerization of A·M**ADP·P_i to A·M′·ADP·P_i, and, consequently, a lower population of force-generating, strongly bound cross-bridges.

Similar arguments on changes in the population of force-generating cross-bridges were presented in a previous study to account for a much reduced *in vitro* motility and force generation with the I341A yeast actin mutant of the strong binding site for myosin (Miller et al., 1996). As shown in that study, and confirmed here by *in vitro* motilities at I = 150 mM, the functional impairment of this mutant, which is greater than that of the weak binding site mutants, occurs at steps subsequent to the weak binding equilibria in Scheme 1 (steps 2 and 4). On the basis of changes in the V_{max} and rigor S1 binding, the mutation of I341 impacts the isomerization (step 5 in Scheme 1) and the strong binding equilibria steps in the cycle. A reduced force is most likely produced because of a decreased isomerization in step 5 and the likely dissociation of myosin from the A·M′·ADP (and A·M·ADP) complex.

Although the loss of the only two N-terminal acidic residues in wild type yeast actin is functionally equivalent to the loss of the D24/D25 or E99/E100 charges, the presence of two additional acidic residues at the N terminus (in the 4Ac mutant), which converts it to an α-actin-like sequence, differentiates this region from the other weak binding sites for myosin. 4Ac actin generates more force with HMM than wild type actin. As in other cases, on the basis of the effects of HMM concentrations on the motilities of 4Ac and WT actins (Table 3), it is assumed that the greater force is related to the increased population of strongly bound states. However, wild type and 4Ac actins have the same weak (Cook et al., 1993) and strong (this work) binding affinities for S1. Thus, the main difference between these two actins, as revealed by V_{max} values of acto-S1 ATPase (Cook et al., 1993), is in the isomerization between the A·M**ADP·P_i and A·M′·ADP·P_i complexes. The improved isomerization with the 4Ac actin increases the flux of HMM into force-generating states of the cycle and yields a greater force than that generated by HMM and wild type actin.

Clearly, our assumptions and conclusions must be verified by optical trap measurements of unitary forces and steps with the actin mutants. At this stage, our results point to a clear distinction between the weak and strong binding sites for myosin on actin. The contribution of these sites to specific steps of the cross-bridge cycle can be evaluated with the help of binding, activity, and motility assays which include variations in load, HMM concentration, and ionic strength conditions. In all of these assays, the charged pairs D24/D25 and E99/E100 are functionally indistinguishable. The first two acidic residues in the N terminus of actin (wild type yeast actin) determine the contribution of this site to S1 binding. The next two acidic residues, as shown for the 4Ac mutant actin, and by implication for α-actin and many other actins, do not improve S1 binding but facilitate the isomerization from A·M**ADP·P_i to A·M′·ADP·P_i and thus the overall flux through the cross-bridge cycle. These distinctions between the different myosin binding sites on actin should be useful in detailed structural modeling of the cross-bridge cycle.

ACKNOWLEDGMENT

We thank Dr. E. Homsher for helpful discussions and comments. We also thank Dr. D. Drubin, D. Botstein, and

K. Wertman for yeast strains Act 1−133 and Act 1−120 (the D24A/D25A and E99A/E100A mutant actin).

REFERENCES

Adams, S., & Reisler, E. (1993) *Biochemistry 32*, 5051−5056.

Bobkov, A. A., Bobkova, E. A., Lin, S. H., & Reisler, E. (1996) *Proc. Natl. Acad. Sci. U.S.A. 93*, 2285−2289.

Botts, J., Muhlrad, A., Takashi, R., & Morales, M. F. (1982) *Biochemistry 21*, 6903−6905.

Brenner, B., Kraft, T., DasGupta, G., & Reisler, E. (1996) *Biophys. J. 70*, 48−56.

Chalovich, J. M., Stein, L. A., Greene, L. E., & Eisenberg, E. (1984) *Biochemistry 23*, 4885−4889.

Chaussepied, P., & Kasprzak, A. A. (1989) *J. Biol. Chem. 264*, 20752−20759.

Cook, R. K., Blake, W. T., & Rubenstein, P. A. (1992) *J. Biol. Chem. 267*, 9430−9436.

Cook, R. K., Root, D., Miller, C., Reisler, E., & Rubenstein, P. A. (1993) *J. Biol. Chem. 268*, 2410−2415.

Crosbie, R. H., Miller, C., Chalovich, J. M., Rubenstein, P. A., & Reisler, E. (1994) *Biochemistry 33*, 3210−3216.

DasGupta, G., & Reisler, E. (1989) *J. Mol. Biol. 207*, 833−836.

DasGupta, G., & Reisler, E. (1991) *Biochemistry 30*, 9961−9966.

DasGupta, G., & Reisler, E. (1992) *Biochemistry 31*, 1836−1841.

Duong, A. M., & Reisler, E. (1987) *J. Biol. Chem. 262*, 4124−4128.

Godfrey, J. E., & Harrington, W. F. (1970) *Biochemistry 9*, 886−895.

Haeberle, J. R. (1994) *J. Biol. Chem. 269*, 12424−12431.

Holmes, K. C. (1995) *Biophys. J. 68*, 2s−7s.

Homsher, E., Wang, F., & Sellers, J. R. (1992) *Am. J. Physiol. 262*, C714−C723.

Johara, M., Toyoshima, Y. Y., Ishijima, A., Kojima, H., Yanagida, T., & Sutoh, K. (1993) *Proc. Natl. Acad. Sci. U.S.A. 90*, 2127−2131.

Kabsch, W., Mannherz, H. G., Suck, D., Pai, E., & Holmes, K. C. (1990) *Nature 347*, 37−44.

Kodama, T., Fukui, K., & Kometani, K. (1986) *J. Biochem. 99*, 1465−1472.

Kraft, T., Chalovich, J. M., Yu, L. C., & Brenner, B. (1995) *Biophys. J. 68*, 2404−2418.

Kron, S. J., Toyoshima, Y. Y., Uyeda, T. Q., & Spudich, J. A. (1991) *Methods Enzymol. 196*, 399−416.

Labbe, J. P., Mornet, D., Roseau, G., & Kassab, R. (1982) *Biochemistry 21*, 6897−6903.

Labbe, J. P., Lelievre, S., Boyer, M., & Benyamin, Y. (1994) *Biochem. J. 299*, 875−879.

Laemlli, U. K. (1970) *Nature 227*, 680−685.

Lionne, C., Brune, M., Webb, M. R., Travers, F., & Berman, T. (1995) *FEBS Lett. 364*, 59−62.

Lymn, R. W., & Taylor, E. W. (1971) *Biochemistry 10*, 4617−4624.

Ma, Y.-Z., & Taylor, E. W. (1994) *Biophys. J. 66*, 1542−1553.

Mejean, C., Boyer, M., Labbe, J. P., Marlier, L., Benyamin, Y., & Roustan, C. (1987) *Biochem. J. 244*, 571−577.

Miller, C. J., & Reisler, E. (1995) *Biochemistry 34*, 2694−2700.

Miller, C. J., Cheung, P., White, P., & Reisler, E. (1995) *Biophys. J. 68*, 50s−54s.

Miller, C. J., Doyle, T., Bobkova, E., Botstein, D., & Reisler, E. (1996) *Biochemistry 35*, 3670-3676.

Miller, L., Kalnoski, M., Yunossi, Z., Bulinski, J. C., & Reisler, E. (1987) *Biochemistry 26*, 6064−6070.

Mornet, D., Pantel, P., Audemard, E., & Kassab, R. (1979) *Biochem. Biophys. Res. Commun. 89*, 925−932.

Rayment, I., Holden, H. M., Whittaker, M., Yohn, C. B., Lorenz, M., Holmes, K. C., & Milligan, R. A. (1993a) *Science 261*, 58−65.

Rayment, I., Rypniewski, W. R., Schmidt-Base, K., Smith, R., Tomchick, D. R., Benning, M. M., Winkelmann, D. A., Wesenberg, G., & Holden, H. M. (1993b) *Science 261*, 50−58.

Regnier, M., Morris, C., & Homsher, E. (1995) *Am. J. Physiol. 269*, C1532−C1539.

Schroder, R. R., Manstein, D. J., Jahn, W., Holden, H., Rayment, I., Holmes, K. C., & Spudich, J. A. (1993) *Nature 364*, 171−174.

Spudich, J. A., & Watt, W. (1971) *J. Biol. Chem. 246*, 4866−4871.

Sutoh, K. (1982) *Biochemistry 21*, 3654−3661.

Sutoh, K., Ando, M., & Toyoshima, Y. Y. (1991) *Proc. Natl. Acad. Sci. U.S.A. 88*, 7711−7714.

Taylor, E. W. (1979) *CRC Crit. Rev. Biochem. 6*, 103−164.

Uyeda, T. Q., Ruppel, K. M., Spudich, J.A. (1994) *Nature 368*, 567−569.

Warrick, H. M., Simmons, R. M., Finer, J. T., Uyeda, T. Q., Chu, S., & Spudich, J. A. (1993) *Methods Cell Biol. 39*, 1−21.

Weeds, A., & Pope, A. B. (1977) *J. Mol. Biol. 111*, 129−157.

Wertman, K. F., Drubin, D. G., & Botstein, D. (1992) *Genetics 132*, 337−350.

Yamamoto, K., & Sekine, T. (1979) *J. Biochem. 86*, 1855−1862.

BI962388+